Frequency conversion, "superluminal" propagation, and compression of a powerful microwave pulse in propagating ionization front

Y. Cao ,[*] Y. P. Bliokh , V. Maksimov, J. G. Leopold , and Ya. E. Krasik
Physics Department, Technion, Haifa 320000, Israel

Frequency up-conversion ($\sim$10%) and compression (almost twofold) of a powerful ($\leqslant$ 250 MW) microwave pulse in the propagating ionization front produced by the pulse itself in a gas-filled waveguide, is investigated experimentally and analyzed theoretically. Pulse envelope reshaping and group velocity increase manifest themselves in a propagation of the pulse faster than in the empty waveguide. A simple one-dimensional mathematical model allows the adequate interpretation of the experimental results.

I. INTRODUCTION

Interest in the propagation of electromagnetic waves in the so-called time-varying media, is not new [1], but attracted renewed attention during the last decade (see, e.g., the review articles [2,3]) because of various potential applications and novel approaches in such media development [4,5]. Currently, experimental and theoretical efforts in this field are concentrated mostly in optics. Various metamaterials are considered as an appropriate medium, whereas initially this function was mainly assigned to plasma. Indeed, propagation of electromagnetic waves in time-varying media was studied theoretically during the second half of the previous century (see Ref. [6] for a historical overview). A major part of these studies dealt with waves propagating in plasma (see, e.g., Ref. [7]). However, despite impressive advances in theory, experiments demonstrated a very modest record of achievements.

In this paper, results of experiments and theoretical modeling of the evolution of an electromagnetic pulse propagating synchronously with the ionization front produced by the pulse itself, are presented. The use of a high-power, about 250 MW, short (0.5 ns) microwave pulse made possible to demonstrate record ($\sim$10%) frequency conversion from 9.5 to 10.5 GHz.

II. SIMPLIFIED THEORETICAL MODEL

Before proceeding to the experiment, let us analyze the expected results and its possible interpretation. An electromagnetic pulse is injected through a transparent window into a gas-filled waveguide. If the microwave pulse power is large enough, the electric fields cause gas discharge producing plasma with rapidly growing density while the ionization front propagates together with the pulse. Thus, each spatial part of the pulse propagates in the plasma, which density is equal to the density at the entrance at the corresponding instant t_0 when this part passed through the window. Here it is assumed that the pulse shape does not change considerably during

propagation. Suppose that the plasma density gradient in the frame of reference of the pulse, is small, $dn/dz^* \ll kn$, then the local frequency $\omega(z^*, t - t_0)$ and the local wave vector $k(z^*, t - t_0)$ of the pulse are connected by the dispersion relation

$$\omega^2 = c^2 k^2 + \omega_{c_0}^2 + \omega_p^2(z^*) \equiv c^2 k^2 + \omega_c^2(z^*). \quad (1)$$

Here z^* is the longitudinal coordinate in the frame of reference of the pulse, ω_{c0} is the cut-off frequency of the empty waveguide, and ω_p is the plasma electron frequency. The wave, the propagation of which in the medium with comoving space- and time-varying parameters is governed by dispersion relation (1), experiences a frequency variation [7,8]

$$\frac{d\omega(t)^2}{dt} = \left. \frac{\partial \omega_c^2}{\partial t} \right|_{t_0}. \quad (2)$$

The derivative d/dt is calculated along the characteristic $z = v_g(t - t_0)$, where v_g is the wave group velocity, and the right-hand side is calculated at the entrance $z = 0$ at time t_0. The plasma frequency growth is described as

$$\frac{\partial \omega_p^2}{\partial t} = \nu \omega_p^2, \quad (3)$$

where ν is the ionization frequency. Equations (2) and (3) show that the wave frequency increases along the wave's path resulting in the increase in the wave group velocity and the latter can exceed the group velocity in the empty waveguide.

The value of the ionization frequency ν depends on the energy $w_e \propto E_0^2$ of electrons, which oscillate in the electric field of amplitude E_0

$$\nu = n_g \langle \sigma_i(w_e)|v_e|\rangle \equiv n_g I(E_0^2), \quad (4)$$

where n_g is the neutral gas density, v_e the electron velocity, $\sigma_i(w_e)$ the ionization cross section, and the chevrons represent averaging over the oscillation period. It follows from Eqs. (2)–(4) that different parts of the pulse experience different frequency shift and, correspondingly, propagate with different group velocities, resulting in the local compression or stretching of the pulse. These equations describe qualitatively the pulse compression and frequency shift, while a

*neo.cao.yang@gmail.com
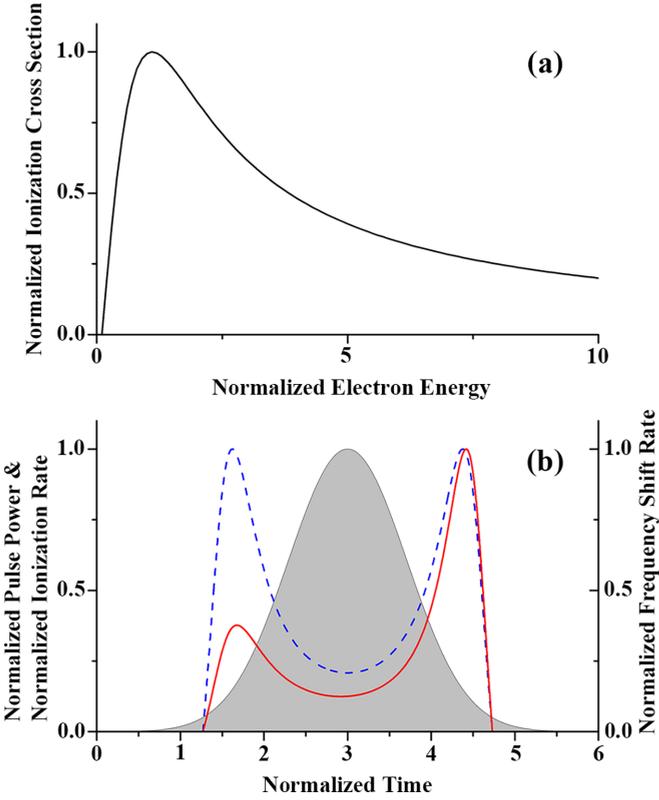
FIG. 1. (a) The electron impact ionization cross section as a function of the electron energy [20]. (b) Normalized electric field amplitude along the pulse (shaded area), the normalized ionization rate (dashed line) and the normalized frequency shift rate (solid line) vs. time.

FIG. 2. Pulse envelope at the waveguide entrance (shaded area), the envelope of the pulse at the waveguide's output end (solid red line), and the trajectories of the pulse layers in time (gray lines).

complete description is challenging. Indeed, the amplitude E_0 of a wave, propagating in the waveguide, is inhomogeneous in the transverse plane resulting in a transverse position, $\vec{r}_\perp$, dependent plasma density. Then, the dispersion Eq. (1) keeps the same form, but the relation between ω_c and $\omega_p(\vec{r}_\perp)$ should include the integral characteristics of the plasma density distribution. Note, that redistribution of the plasma density in the transverse plane, on its own, leads to wave frequency shift [9]. Next, the compressing/stretching changes the pulse envelope along the propagation path, while Eq. (2) in combination with Eq. (3) is valid when these changes are neglected. Also, Eqs. (1) and (2) should be supplemented with equations that describe evolution of the cut-off frequency $\omega_c(t)$. Nevertheless, despite these complications, the experimental results described below are evidence that the combined propagation of the pulse and the ionization front can be described by Eqs. (1)–(3) quite well.

The electron impact ionization cross section, Fig. 1(a), depends nonmonotonically on the electron energy [10]. The energy of the oscillating electron is defined by a local power of an electromagnetic pulse. When the maximum pulse power is so large that the electron energy exceeds significantly the energy corresponding to the maximum ionization cross section, the ionization rate at the temporal center of the pulse can be much smaller than at its leading and rear parts. Consequently, the ionization rate $I[(E_0^2(z^*)]$ is a two-humped shape curve

when considered along the pulse [Fig. 1(b)]. When the dip in the ionization rate is sufficiently deep, the time dependence of the rate of the pulse's local frequency shift is also characterized by two local maxima [Fig. 1(b)]. The second maximum, is always higher than the first, because the rate of the plasma generation is proportional to the plasma density which is an increasing function of time.

Whether the shape of the ionization rate is two-humped or not, the rear part of the pulse experiences larger frequency up-shift than the leading part resulting in that the rear part of the pulse moves faster than the leading part, which leads to compression of the pulse. Note that reshaping of the pulse's envelope can lead to an apparent propagation velocity exceeding even the speed of light in vacuum [11,12].

Let the pulse amplitude $E_0(t, z)$, local frequency $\omega(t, z)$, local group velocity $v_g(z, t)$ and plasma density $n(z, t)$ at some distance z be known for time $-\infty < t < \infty$. It is desired to find all these quantities at a distance $z + \Delta z$. Let us represent the pulse at point z as a set of discrete numbered time layers, each following the other along time and characterized by its own amplitude, frequency, and group velocity. Layer i, propagating along the distance Δz, produces an additional plasma density Δn_i during the propagation time $\Delta t_i = \Delta z / v_{g_i}$, as described by Eqs. (3) and (4). Assuming that this additional density is distributed uniformly along the distance Δz, a new plasma density temporal sampling at the point $z + \Delta z$ is obtained. It is important that the new sampling is given at nonequidistant points in time $t_i' = t_i + \Delta t_i$, even when the sampling was equidistant at point z. By virtue of the energy conservation law, the new amplitude of the wave in layer i either increases or decreases depending on whether the new sampling is compressed or stretched. The new frequency is calculated using Eq. (2) and the density's temporal profile at point $z + \Delta z$. Next, using $z + \Delta z$ as a new starting point, the pulse parameters and the plasma density at $z + 2\Delta z$ are calculated, and so on. Evolution of the pulse envelope and trajectories of the pulse layers are shown in Fig. 2.

III. EXPERIMENTAL SETUP AND DIAGNOSTICS

In Fig. 3, a sketch of the experimental setup used is shown. The high-power microwave (HPM) pulse (power $\sim$ 250 MW, duration $\sim$0.5 ns, carrier frequency $\sim$9.5 GHz, TM$_{01}$ mode)
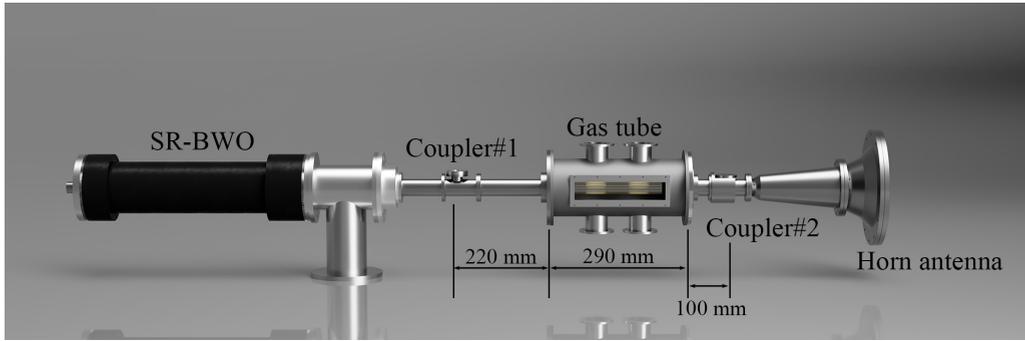
FIG. 3. Sketch of the experimental setup.

is produced by a superradiant backward wave oscillator (SR-BWO) (see [13,14] for detail).

A 28-mm-diameter circular waveguide is connected at the output of the SR-BWO with a calibrated coupler (#1) [15] at its center. This is followed by the gas tube, filled with helium or air at the desired pressure. Inside the gas tube, the HPM pulse propagates in a 28-mm-diameter solid-wall waveguide with 2-mm-diameter drilled holes for gas filling. A second calibrated coupler (#2) is connected at the exit from the gas tube followed by an impedance-matched horn antenna. Couplers #1 and #2 measure the incident, transmitted, and reflected wave forms acquired by an Agilent DSO81204B oscilloscope (12 GHz, 40 Gs/s). At the entrance and exit of the gas tube, a 0.3-mm-thick Mylar interface window is installed to isolate the vacuum/gas/vacuum media.

IV. EXPERIMENTAL RESULTS

Transmitted microwave power wave forms in helium within the pressure range $10^{-4}-12$ Torr are shown in Fig. 4(a). The wave forms are averaged over 10 shots and each transmitted wave form is normalized to the maximum of the corresponding incident power wave form. One can see that at $P < 6.5$ Torr the transmitted power is similar to that obtained at $P = 10^{-4}$ Torr. Within the pressure range 7.5–8.5 Torr, transmitted power wave forms show significant (up to 50%) compression and power of up to 100% higher than the

incident pulse power. At higher pressures, although the power and width decrease significantly, the pulse propagates faster than in an empty waveguide.

The dependence of the transmission coefficient, η, defined as the ratio between the peak transmitted and incident power on helium pressure, is shown in Fig. 4(b). One can see that the value of η remains almost unchanged up to $P = 7$ Torr and a sharp increase in η is observed in the narrow range of pressure, $P = 7.5$–8.5 Torr. The value of η decreases when $P > 8.5$ Torr, approaching almost zero for $P > 11$ Torr. The increase in value of η is to be related to the pulse compression seen in Fig. 4(a). The decrease in η as the pressure increases is the result of pulse energy losses due to increased ionization/excitation frequency and plasma electron heating. Similar results were obtained for air. For air, the range of pressures where $1 < \eta < 1.2$, was obtained for $1.4 \leqslant P \leqslant 1.6$ Torr and at $P > 3$ Torr the transmitted pulse power becomes negligible.

In Figs. 5(a) and 5(b), the transmitted normalized pulse power wave forms exiting from vacuum and from $P = 8$ Torr helium, respectively, are presented. Whereas in vacuum the central frequency is $f_c \approx 9.5$ GHz [Fig. 5(c)], in $P = 8$ Torr, the spectrum becomes broader with central frequency at $f_c \approx 10.5$ GHz and the frequency upshift at the pulse tail is higher than that at its front. The latter demonstrates pulse self-compression caused by fast ionization within the pulse as suggested by the theoretical model. Figure 4(a) demon-
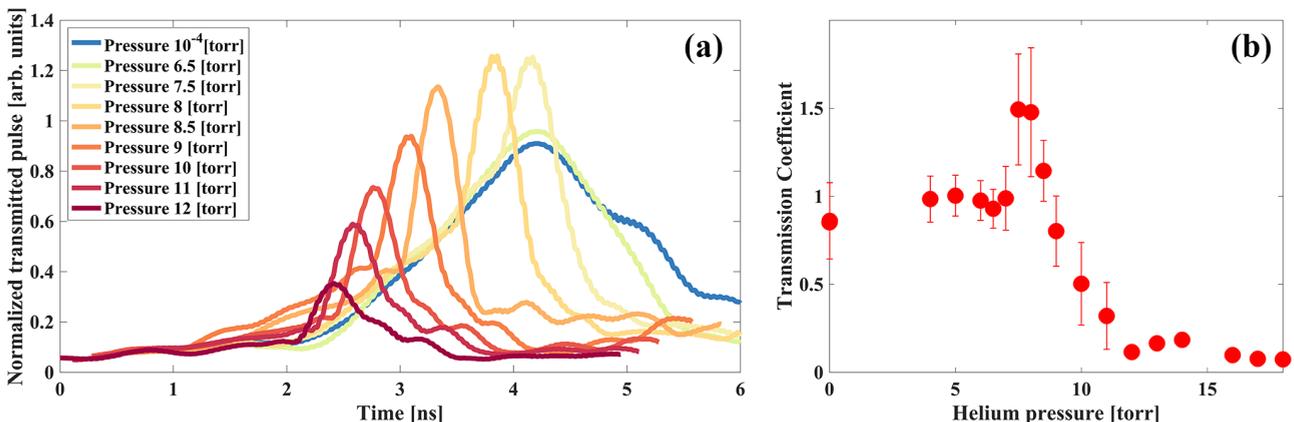
FIG. 4. (a) The transmitted microwave power envelopes obtained at different pressures in a helium-filled cylindrical waveguide (average of 10 pulses); (b) The dependence of the transmission coefficient on helium pressure.
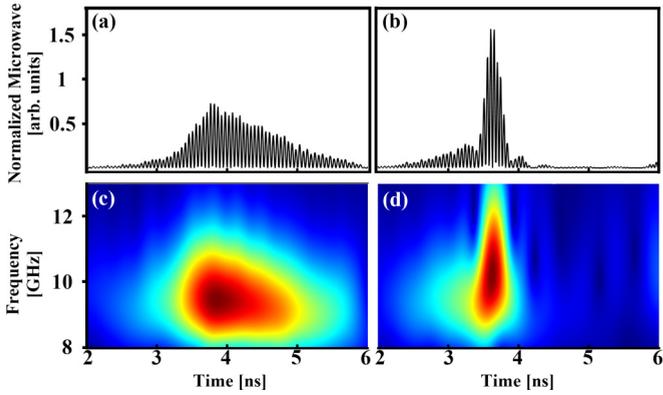
FIG. 5. The transmitted HPM pulse in vacuum (a) and in P = 8 Torr helium (b) and their the time-frequency analysis in (c) and (d) respectively.

strates the "superluminal" propagation of the pulse at pressure ⩾8 Torr.

Comparison of the local dominant frequency variations along the incoming and outgoing pulses is shown in Fig. 6. The frequency shift in the outgoing pulse is a two-humped shape with a dominant second maximum similar to the behavior seen in Fig. 1(b). It is necessary to note that this phenomenon is peculiar feature of microwave gas discharge, when electron impact ionization is the main mechanism of the plasma formation, while in the optics frequency range this is photoionization. The photoionization cross section, in contrast to the impact ionization, is independent of the electromagnetic wave amplitude.

The frequency spectrum of the incoming pulse is rather broad [see Fig. 5(c)] so that the dispersion can change the
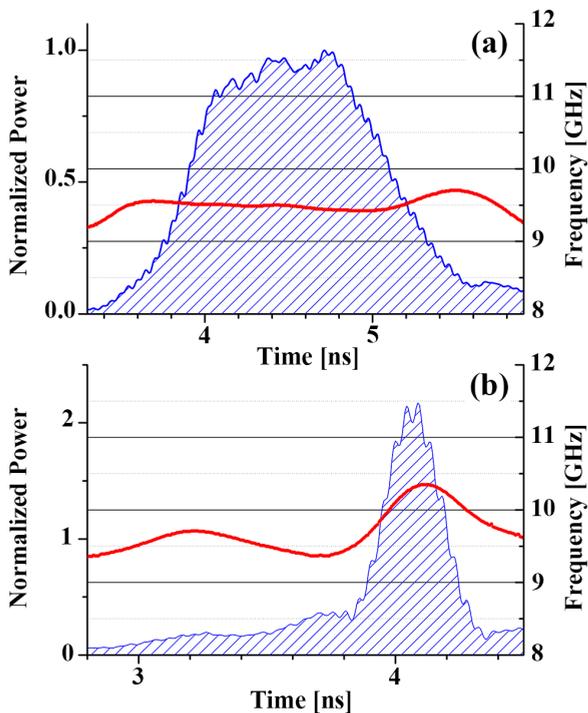
FIG. 6. Wave form (shaded area) and local frequency (solid red line) of the incoming (a) and outgoing (b) pulses for 8 Torr helium.
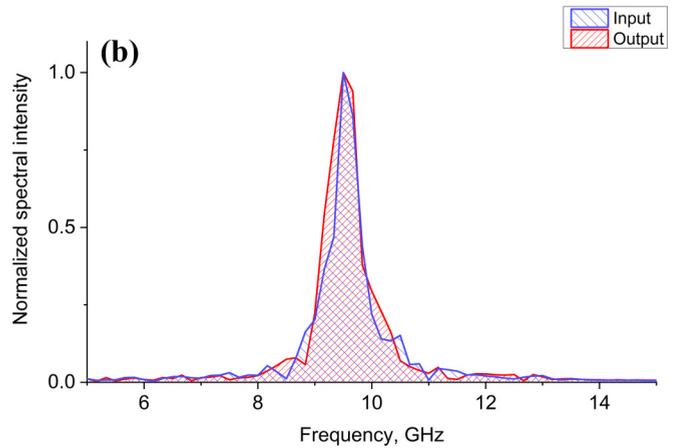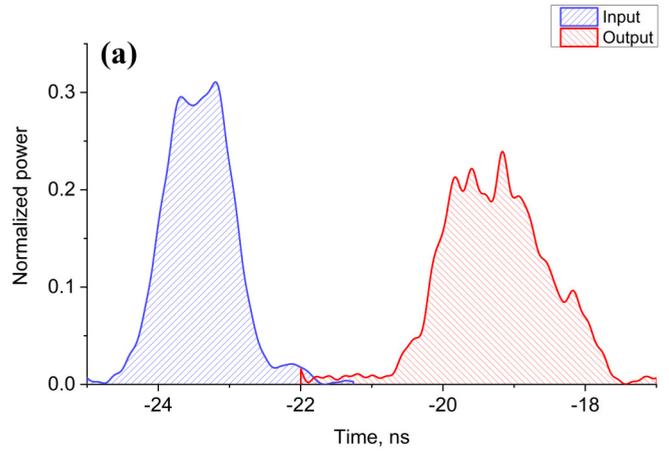
FIG. 7. (a) Normalized power of the incoming (blue line) and outgoing (shaded area) pulses in the empty waveguide; (b) Frequency spectra of incoming and outgoing pulses.

envelope of the pulse during its propagation in the empty waveguide, while the spectrum remains unchanged. Indeed, propagation in the empty waveguide leads to increase of the pulse duration and decrease of the maximum power, as it is shown in Fig. 7(a). However, the spectra of signals obtained by the couplers #1 (incoming signal) and #2 (outgoing signal) are practically identical [see Fig. 7(b)]. This behavior is in contrast to that realized for the pulse propagation in the co-moving ionization front. In addition, it should be emphasized that 290-mm-long waveguide insert filled with gas not only compensates the dispersion-induced spread of the pulse, but leads to the pulse compression as well.

V. SUMMARY

In this paper the propagation of a powerful short microwave pulse in a nonstationary and nonuniform medium with time varying parameters is studied both experimentally and theoretically. The ionization front, produced by the microwave pulse itself in a gas-filled waveguide and the plasma density being the time varying parameter of the medium, propagates synchronously with the pulse. The resulting specific phenomena, that is, frequency conversion and pulse compression have been demonstrated experimentally.

Observed relative frequency shift $\Delta f/f \sim 10\%$ far exceeds obtained previously experimental results $\Delta f/f \sim 0.1\%$ in the microwave frequency range [16,17] and the resent result $\Delta f/f \sim 4\%$ in optics ($\lambda \approx 1.3\mu$) [18]. In the microwave experiments, only $\sim 0.1\%$ frequency shift is related to small (~ 1 MW in Ref. [16] and ~ 250 kW in Ref. [17]) microwave power. Moreover, the microwave beams in these experiments were radiated by horn antennas, so that the wave amplitude decreased with the distance. As a result, the plasma density n grows very slow, whereas the frequency shift is proportional to dn/dt. Increasing the microwave power by several orders of magnitude and eliminating the angular divergence allow us to reach the results described above.

[1] Yu. A. Kravtsov and Yu. I. Orlov, *Geometrical Optics of Inhomogeneous Media* (Springer-Verlag, Berlin, 1990).

[2] D. L. Sounas and A. Alú, Nat. Photonics **11**, 774 (2017).

[3] E. Galiffi, R. Tirole, S. Yin, H. Li, S. Vezzoli, P. A. Huidobro, M. G. Silveirinha, R. Sapienza, A. Alú, and J. Pendry, Adv. Photonics **4**, 014002 (2022).

[4] Christophe Caloz and Zoé-Lise Deck-Léger, IEEE Trans. Antennas Propag. **68**, 1569 (2020).

[5] N. Engheta, Nanophotonics **10**, 639 (2021).

[6] G. A. Ptitcyn, M. S. Mirmoosa, A. Sotoodehfar, and S. A. Tretyakov, arXiv:2211.13054.

[7] N. S. Stepanov, Radiophys. Quantum Electron. **11**, 394 (1968).

[8] L. A. Ostrovsky, Izvestiya Vysshikh Uchebnykh Zavedenii, Radiofizika **4**, 293 (1961).

[9] Y. Cao, Y. P. Bliokh, J. G. Leopold, A. Li, G. Leibovitch, and Ya. E. Krasik, Phys. Plasmas **27**, 053103 (2020).

[10] Y. Ralchenko, R. K. Janev, T. Kato, D. V. Fursa, I. Bray, and F. J. de Heer, Data Nuclear Data Tables **94**, 603 (2008).

[11] L. Brillouin, *Wave Propagation and Group Velocity* (Academic, New York, 1960).

[12] L. A. Vainstein, Sov. Phys. Usp. **19**, 189 (1976).

[13] A. Eltchaninov, S. D. Korovin, G. A. Mesyats, I. V. Pegel, V. V. Rostov, V. G. Shpak, and M. I. Yalandin, IEEE Trans. Plasma Sci. **32**, 1093 (2004).

[14] V. V. Rostov, I. v. Romanchenko, M. S. Pedos, S. N. Rukin, K. A. Sharypov, V. G. Shpak, S. A. Shunailov, M. R. Ul'Masculov, and M. I. Yalandin, Phys. Plasmas **23**, 093103 (2016).

[15] L. M. Earley, W. P. Ballard, and C. B. Wharton, IEEE Trans. Nucl. Sci. **32**, 2921 (1985).

[16] S. P. Kuo and A. Ren, J. Appl. Phys. **71**, 5376 (1992).

[17] B. Cros, X. Xu, T. Tsukada, N. Yugami, Y. Nishida, and G. Matthieussent, Phys. Plasmas **4**, 2837 (1997).

[18] K. Pang, M. Z. Alam, Y. Zhou *et al.*, Nano Lett. **21**, 5907 (2021).